

**The Variable Stars from the OGLE-III Shallow Survey  
in the Large Magellanic Cloud\***K. Ulaczyk<sup>1</sup>, M.K. Szymański<sup>1</sup>, A. Udalski<sup>1</sup>,  
M. Kubiak<sup>1</sup>, G. Pietrzyński<sup>1,2</sup>, I. Soszyński<sup>1</sup>,  
Ł. Wyrzykowski<sup>1,3</sup>, R. Poleski<sup>1,4</sup>,  
W. Gieren<sup>2</sup>, A.R. Walker<sup>5</sup> and A. Garcia-Varela<sup>6</sup><sup>1</sup>Warsaw University Observatory, Al. Ujazdowskie 4, 00-478 Warszawa, Poland  
e-mail: (kulaczyk,msz,udalski,mk,pietrzyn,soszynsk,wyrzykow,rpoleski)@astrouw.edu.pl<sup>2</sup>Universidad de Concepción, Departamento de Astronomía, Casilla 160-C, Concepción,  
Chile

e-mail: wgieren@astro-udec.cl

<sup>3</sup>Institute of Astronomy, University of Cambridge, Madingley Road, Cambridge  
CB3 0HA, UK<sup>4</sup>Department of Astronomy, The Ohio State University, 140 W. 18th Ave., Columbus, OH  
43210, USA<sup>5</sup>Cerro Tololo Inter-American Observatory, Casilla 603, La Serena, Chile  
e-mail: awalker@ctio.noao.edu<sup>6</sup>Departamento de Física, Universidad de los Andes, Bogota, Colombia  
e-mail: josegarc@uniandes.edu.co*Received March 21, 2013***ABSTRACT**

We describe variable stars found in the data collected during the OGLE-III Shallow Survey covering the *I*-band magnitude range from 9.7 mag to 14.5 mag. The main result is the extension of period–luminosity relations for Cepheids up to 134 days. We also detected 82 binary systems and 110 long-period variables not present in the main OGLE catalogs. Additionally 558 objects were selected as candidates for miscellaneous variables.

**Key words:** *Magellanic Clouds – Surveys – Catalogs – Cepheids – Stars: late type – binaries: eclipsing variables*

**1. Introduction**

In the previous paper (Ulaczyk *et al.* 2012) we described reduction procedures applied to the data obtained in the course of the OGLE-III Shallow Survey in the

---

\*Based on observations obtained with the 1.3 m Warsaw telescope at the Las Campanas Observatory of the Carnegie Institution for Science.

Large Magellanic Cloud. We have also published photometric maps and discussed the quality of photometric data.

Here we present results of variability search based on the same survey. So far most numerous and extensive catalogs of variable stars for that galaxy were published based on the OGLE-III data (*e.g.*, Soszyński *et al.* 2008, 2009a, 2009b). In order to improve even further their completeness we decided to include bright variable objects of luminosities up to the Shallow Survey saturation *I*-magnitude of 9.3. The main purpose was to supplement the OGLE-III catalogs with bright Cepheids to derive consistent luminosity–period relations for wider range of periods. The survey was also focused on red giant variables and luminous eclipsing stars. In the following sections we describe subsequent types of identified variable stars.

## 2. Observational Data

As it was described in the previous paper photometric data were collected using the 1.3-m Warsaw Telescope located at Las Campanas Observatory, operated by the Carnegie Institution for Science. The mosaic camera consisted of eight CCD chips covering approximately  $35' \times 35'$  field of view with the scale of 0.26 arc-sec/pixel. Observations were evenly carried out through the *I* and *V* filters closely resembling standard filters, although the *I*-band filter had higher transmission for longer wavelengths, which was appropriately corrected during the reductions based on calibrated OGLE-IV photometry (Szymański *et al.* 2011). We used exactly the same photometric system as in the OGLE-III main survey. Detailed information about whole instrumentation can be found in Udalski (2003).

Images were collected during the nights of seeing worse than about  $2''$ . It allowed to blur profiles of the brightest stars preventing them from saturation. Moreover, we were able to perform observations during the nights of poor weather which normally would be lost for the main OGLE survey. Details on reduction procedures were described in the previous paper (Ulaczyk *et al.* 2012).

## 3. Variability Search

Using FNPEAKS program created by Z. Kołaczkowski we calculated power spectrum of periods for 65 989 stars having over 10 observational points and with average *I*-band magnitude brighter than 14.5 mag. The frequency range from 0.002 to 2 cycles per day was tested with a step of 0.00001. For every star highest peaks were selected and all objects with signal-to-noise values higher than 3–4, depending on number of observational points, were visually examined. Due to limited number of measurements power spectra were prone to display periodicities around 1-day corresponding to observation sampling, so plenty of objects had to be rejected. The remaining stars were classified into the main variability types – Cepheid variables, RR Lyr variables, eclipsing binaries, long-period variables – and a group of miscellaneous variables.

#### 4. Classical Cepheids

In the main OGLE-III catalog (Soszyński *et al.* 2008) 26 bright fundamental-mode Cepheids in the LMC were saturated at least in one filter while five objects were saturated in both filters. It prevented Soszyński *et al.* (2008) from including them in the complete period–luminosity analysis. Only 21 objects from that sample in the  $V$ -band relation were used and the relation shows significant scatter. The Shallow Survey allowed us to obtain good quality  $VI$  photometry for these Cepheids. Also two completely new Cepheid variables were found with BRIGHT-CEP-1 object apparently belonging to the NGC 1698 star cluster. They were omitted in the main catalog due to the location close to the saturated objects masked out on the OGLE-III reference image. Fig. 1 presents the color–magnitude diagram for

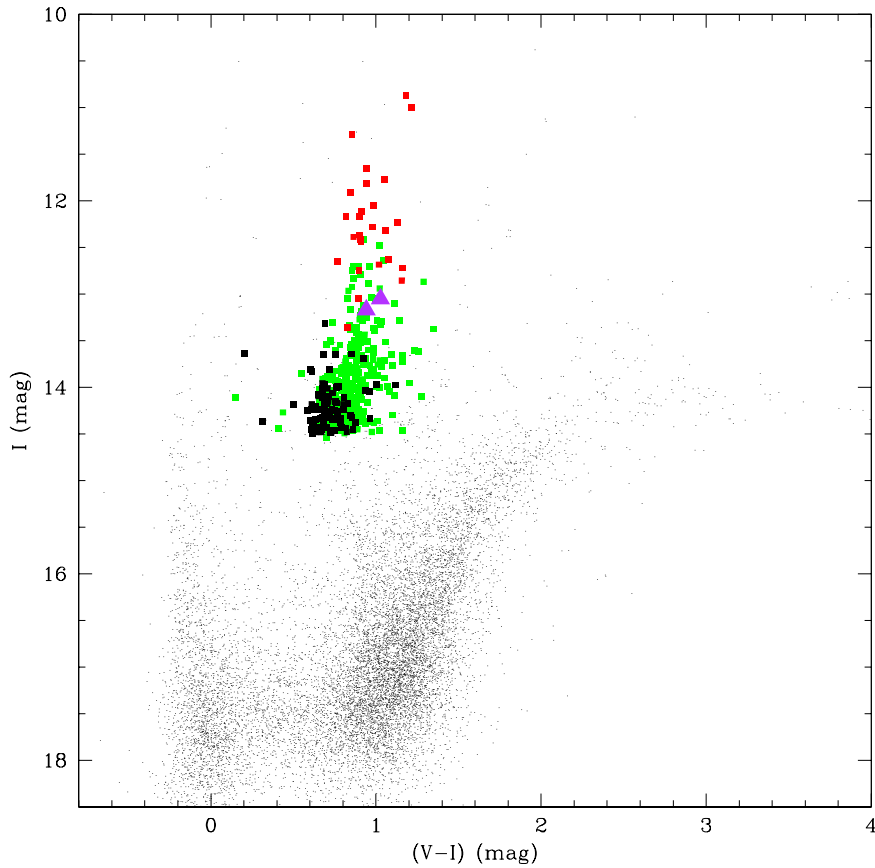


Fig. 1. Color–magnitude diagram for Cepheids. Red points correspond to stars for which new photometry was obtained and violet triangles correspond to newly found objects. Fundamental-mode pulsators from the OGLE-III catalog are marked with green points and secondary-mode pulsators (mostly first overtone) with black points. All measurements are from the Shallow Survey.

all Cepheids classified in the survey with emphasizing the objects for which photometric data were not available or were incomplete. We also show the *VI*-band light curves in Figs. 2–5. The light curve of OGLE-LMC-CEP-0619 variable appears to have additional structure. We subtracted dominant period in both bands but the results are inconclusive. The comparison with the ASAS<sup>†</sup> (Pojmański 2002) data suggests that its amplitude is modulated.

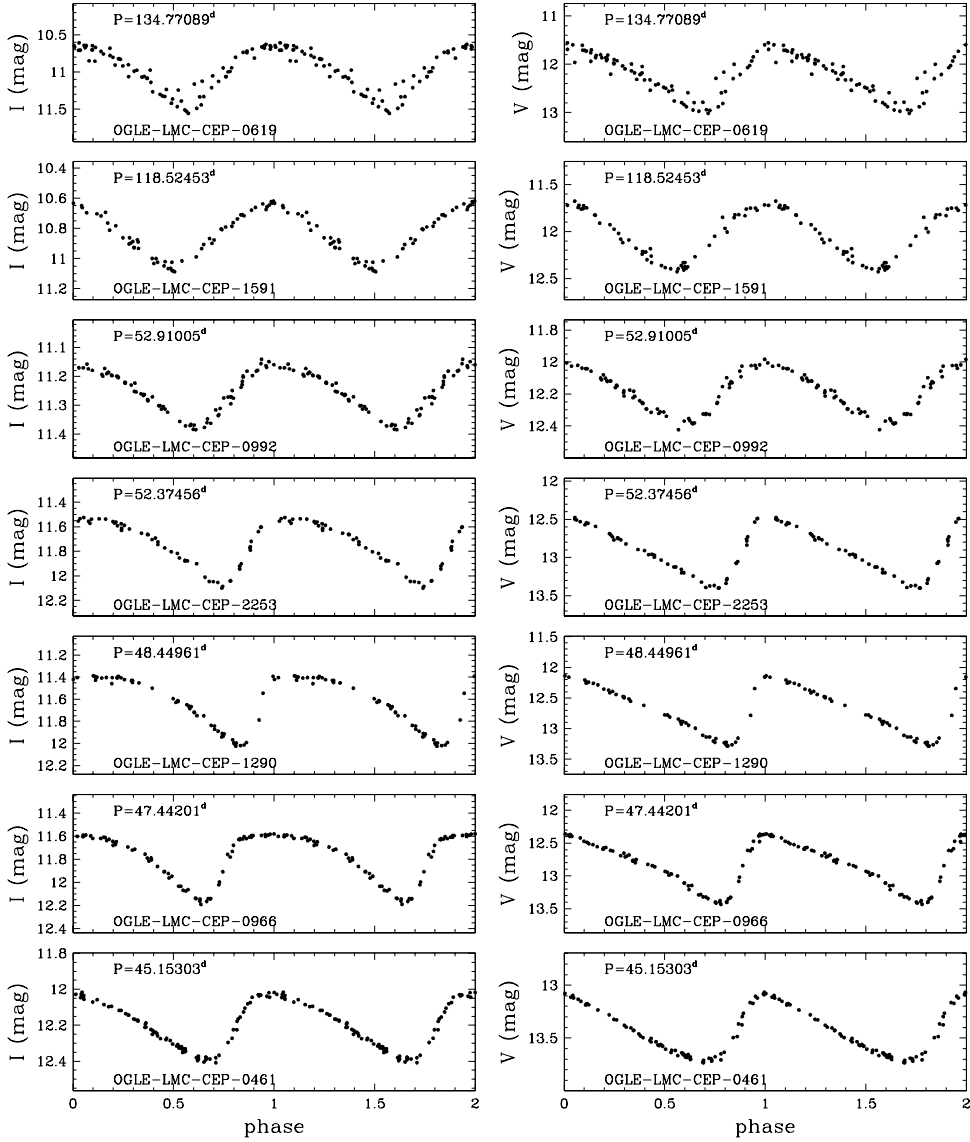


Fig. 2. *VI*-band light curves of Cepheids for which new photometry was obtained, sorted according to decreasing period (periods range 135 to 45 days).

<sup>†</sup><http://www.astrouw.edu.pl/asas/>

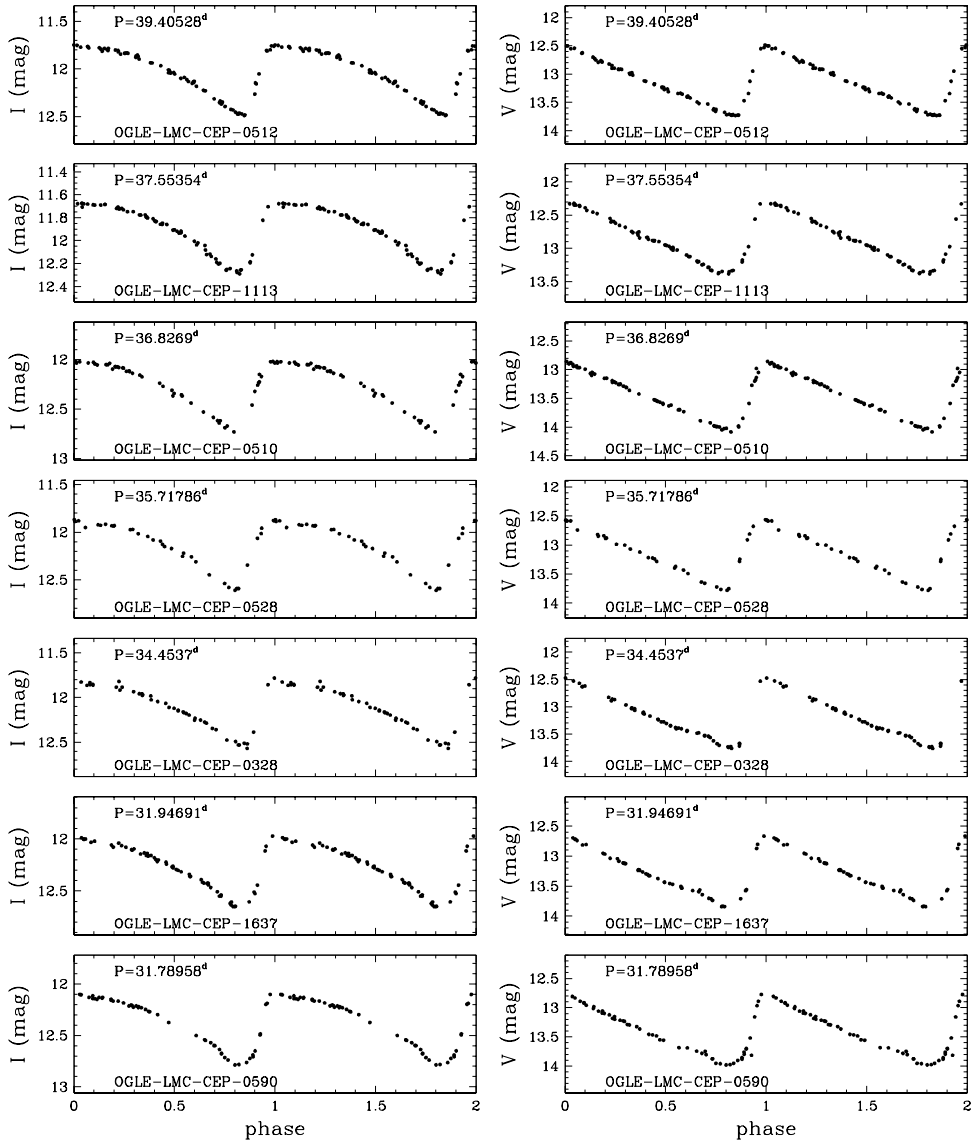


Fig. 3. *VI*-band light curves of Cepheids for which new photometry was obtained, sorted according to decreasing period (periods range 40 to 31 days).

In the observed fields 11 of total 416 objects already present in the OGLE-III catalogs in the range of analyzed magnitudes were overlooked by the Shallow Survey search procedure mainly due to localization close to the detector edge or small amplitudes of variability combined with limited number of observational points. For each object Fourier series with eight harmonics was fitted to the folded *VI* light curves and mean magnitudes were derived by integration of light curves in intensity units. Fig. 6 presents Fourier coefficients  $R_{21}$ ,  $R_{31}$ ,  $\phi_{21}$  and  $\phi_{31}$  as a function of the period, where amplitude ratios  $R_{k1} = A_k/A_1$  and phase differences  $\phi_{k1} = \phi_k - k\phi_1$ .

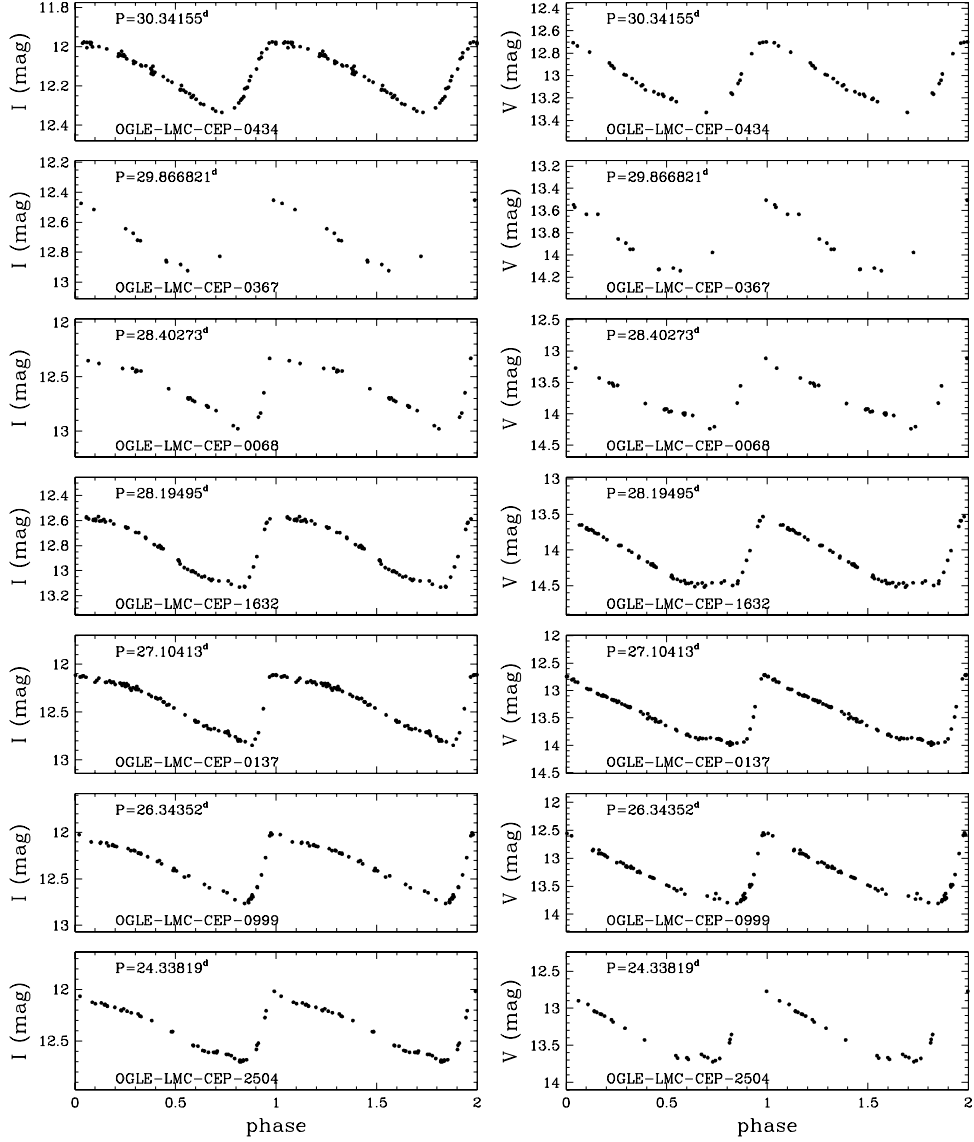


Fig. 4. VI-band light curves of Cepheids for which new photometry was obtained, sorted according to decreasing period (periods range 31 to 24 days).

Table 1 contains basic parameters for each Cepheid. In the subsequent columns the following data are presented: (1) variable star identification label (new objects have prefix “BRIGHT”), (2,3) equatorial coordinates J2000.0, (4) subfield designation, (5) period, (6) *I*-band mean magnitude, (7) *V*-band mean magnitude, (8) (*V*-*I*) color index, (9-14) Fourier parameters for the *I*-band curve, (15-20) Fourier parameters for the *V*-band curve, (21) number of observations in the *I*-band, (22) number of observations in the *V*-band.

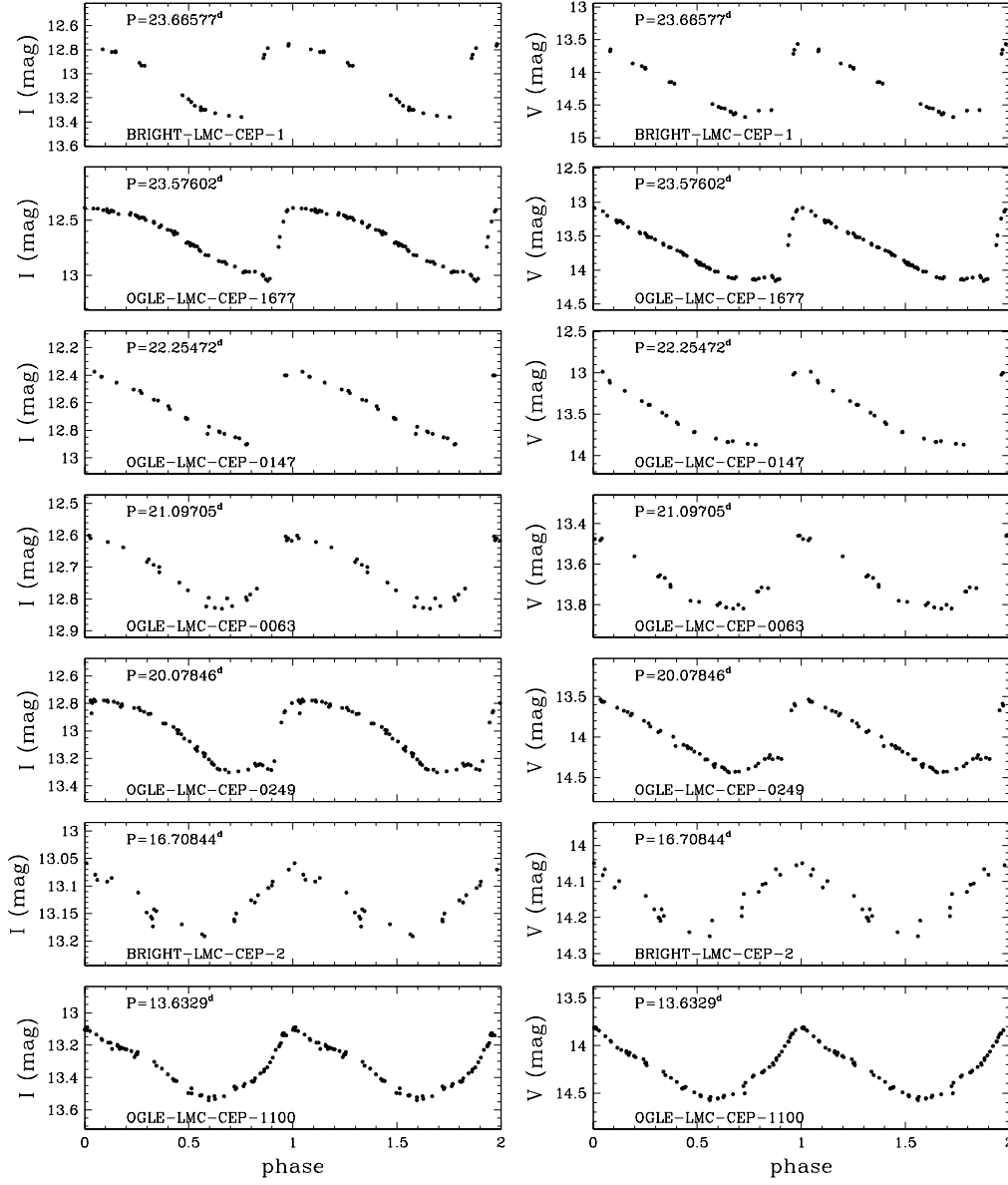


Fig. 5. VI-band light curves of Cepheids for which new photometry was obtained, sorted according to decreasing period (periods range 24 to 13 days).

For fundamental-mode pulsators with periods longer than 10 days  $\log P-I$  and  $\log P-W_I$  relations were fitted using the least squares method with  $3\sigma$  clipping:

$$\begin{aligned} W_I &= -3.294(\pm 0.050) \log P + 15.847(\pm 0.063) & \sigma &= 0.118 \\ I &= -2.984(\pm 0.085) \log P + 16.924(\pm 0.108) & \sigma &= 0.200 \end{aligned} \quad (1)$$

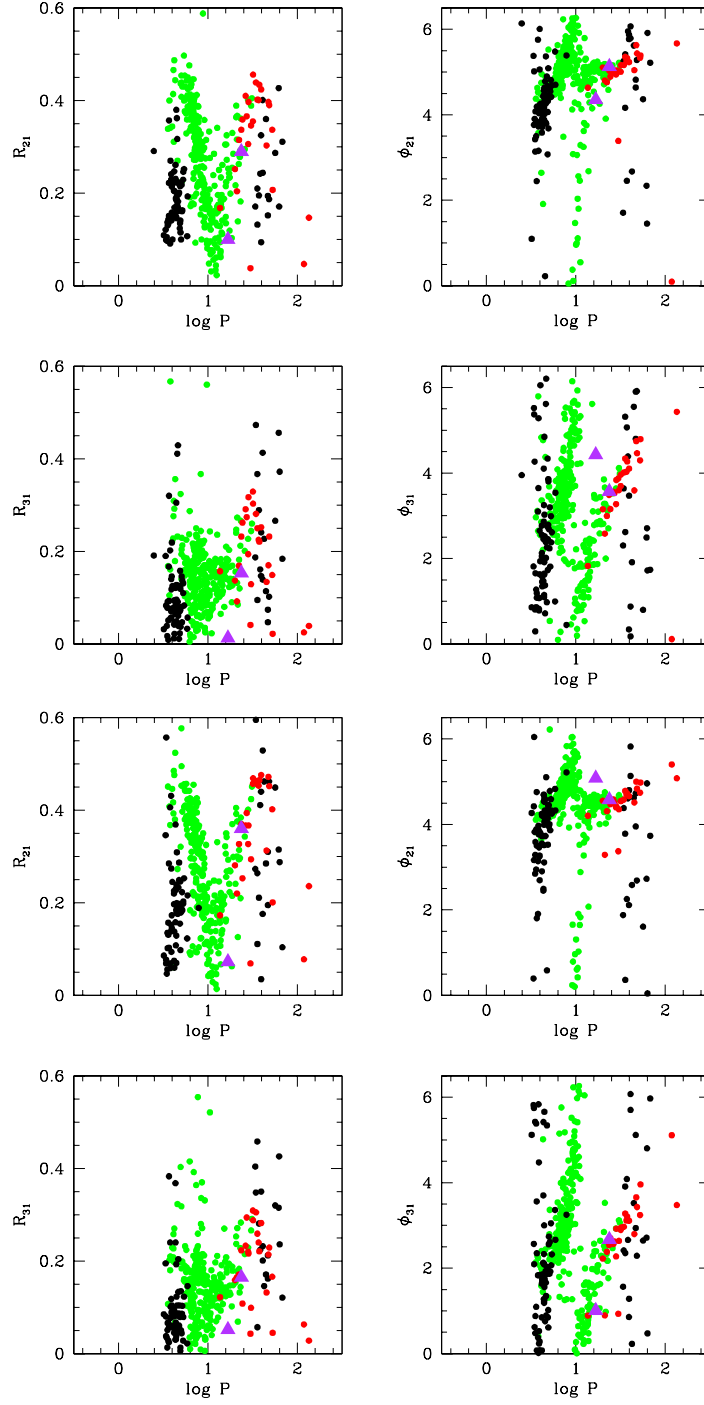


Fig. 6. Fourier parameters for Cepheids. Red points represent objects with new photometry and violet triangles are new Cepheids. Fundamental-mode pulsators from the OGLE-III survey are marked with green color. Black dots are Cepheids pulsating in non-fundamental modes. *Four upper panels* are for *I*-band and the *lower ones* are for *V*-band. All measurements are from the Shallow Survey.



Table 1

Basic parameters of Cepheids derived with OGLE Shallow Survey photometry

ID	RA (J2000.0)	DEC (J2000.0)	Subfield	Period [days]	$I$ [mag]	$V$ [mag]	$V - I$ [mag]	$I$ -band light curve						$V$ -band light curve						$N_I$	$N_V$
								$T_{\max}$ [HJD-2450000]	$A$	$R_{21}$	$\phi_{21}$	$R_{31}$	$\phi_{31}$	$T_{\max}$ [HJD-2450000]	$A$	$R_{21}$	$\phi_{21}$	$R_{31}$	$\phi_{31}$		
BRIGHT-LMC-CEP-1	4 <sup>h</sup> 49 <sup>m</sup> 04.5 <sup>s</sup>	-69°06'43"	LMC142.3	23.66577	13.050	14.077	1.027	4345.69600	0.60	0.289	5.113	0.158	3.550	4343.25225	1.08	0.360	4.582	0.165	2.671	24	25
BRIGHT-LMC-CEP-2	4 <sup>h</sup> 46 <sup>m</sup> 08.4 <sup>s</sup>	-69°02'47"	LMC142.5	16.70844	13.169	14.110	0.941	4359.42193	0.13	0.100	4.358	0.013	4.430	4359.49039	0.20	0.073	5.081	0.052	1.005	25	24
OGLE-LMC-CEP-0063	4 <sup>h</sup> 45 <sup>m</sup> 18.7 <sup>s</sup>	-69°16'38"	LMC142.7	21.09705	12.745	13.624	0.879	4348.21410	0.21	0.204	4.804	0.092	2.581	4326.83017	0.35	0.195	3.968	0.099	2.025	25	23
OGLE-LMC-CEP-0068	4 <sup>h</sup> 45 <sup>m</sup> 37.2 <sup>s</sup>	-70°15'04"	LMC144.4	28.40273	12.633	13.706	1.073	4359.54071	0.65	0.397	5.038	0.317	3.837	4333.19359	1.08	0.366	4.421	0.215	2.918	25	23
OGLE-LMC-CEP-0137	4 <sup>h</sup> 49 <sup>m</sup> 53.8 <sup>s</sup>	-69°45'16"	LMC136.6	27.10413	12.441	13.348	0.907	3231.96866	0.78	0.366	4.980	0.274	3.534	3231.88067	1.33	0.394	4.496	0.294	2.623	77	76
OGLE-LMC-CEP-0147	4 <sup>h</sup> 50 <sup>m</sup> 03.2 <sup>s</sup>	-68°15'34"	LMC140.1	22.25472	12.649	13.416	0.767	4332.13835	0.52	0.315	4.763	0.169	2.995	4354.40310	0.92	0.327	4.311	0.171	2.381	25	21
OGLE-LMC-CEP-0249	4 <sup>h</sup> 52 <sup>m</sup> 47.7 <sup>s</sup>	-68°20'56"	LMC133.8	20.07846	13.048	13.946	0.898	3223.26276	0.55	0.252	5.108	0.137	3.155	3223.11134	0.94	0.281	4.553	0.153	2.226	57	47
OGLE-LMC-CEP-0328	4 <sup>h</sup> 54 <sup>m</sup> 23.9 <sup>s</sup>	-70°54'05"	LMC130.6	34.45370	12.114	13.027	0.913	3275.00059	0.75	0.439	5.163	0.281	4.012	3309.25352	1.30	0.463	4.582	0.305	2.966	44	50
OGLE-LMC-CEP-0367	4 <sup>h</sup> 55 <sup>m</sup> 06.3 <sup>s</sup>	-67°28'33"	LMC132.2	29.86682	12.734	13.890	1.156	4338.43101	0.46	0.111	4.368	0.055	1.220	4338.21500	0.62	0.095	3.681	0.077	0.641	12	14
OGLE-LMC-CEP-0434	4 <sup>h</sup> 56 <sup>m</sup> 27.5 <sup>s</sup>	-69°22'46"	LMC127.7	30.34155	12.164	12.980	0.816	3235.06302	0.36	0.346	5.016	0.129	3.598	3295.83287	0.63	0.294	4.354	0.099	2.639	69	32
OGLE-LMC-CEP-0461	4 <sup>h</sup> 57 <sup>m</sup> 01.8 <sup>s</sup>	-67°59'43"	LMC133.3	45.15303	12.232	13.363	1.131	3202.10571	0.36	0.303	5.045	0.134	3.593	3198.96320	0.64	0.313	4.513	0.132	2.798	86	74
OGLE-LMC-CEP-0510	4 <sup>h</sup> 58 <sup>m</sup> 05.6 <sup>s</sup>	-69°27'15"	LMC127.8	36.82690	12.318	13.374	1.056	3225.80352	0.72	0.401	5.260	0.225	4.028	3224.73503	1.20	0.453	4.705	0.240	3.114	50	63
OGLE-LMC-CEP-0512	4 <sup>h</sup> 58 <sup>m</sup> 10.8 <sup>s</sup>	-69°56'59"	LMC128.7	39.40528	12.046	13.031	0.985	3224.19225	0.73	0.424	5.233	0.252	4.101	3223.68992	1.24	0.476	4.661	0.282	3.109	73	69
OGLE-LMC-CEP-0528	4 <sup>h</sup> 58 <sup>m</sup> 32.8 <sup>s</sup>	-70°20'45"	LMC129.3	35.71786	12.166	13.064	0.898	3298.51189	0.73	0.402	5.356	0.250	4.337	3369.78102	1.22	0.456	4.785	0.259	3.277	35	34
OGLE-LMC-CEP-0590	4 <sup>h</sup> 59 <sup>m</sup> 41.2 <sup>s</sup>	-69°27'21"	LMC127.1	31.78958	12.411	13.314	0.903	3231.96580	0.73	0.355	5.006	0.329	3.694	3327.33092	1.30	0.456	4.540	0.309	2.881	51	54
OGLE-LMC-CEP-0619	5 <sup>h</sup> 00 <sup>m</sup> 07.6 <sup>s</sup>	-68°26'60"	LMC126.4	134.77089	11.005	12.218	1.213	3235.04996	0.80	0.147	5.670	0.039	5.431	3214.64903	1.29	0.236	5.080	0.028	3.476	77	71
OGLE-LMC-CEP-0966	5 <sup>h</sup> 06 <sup>m</sup> 48.0 <sup>s</sup>	-70°02'13"	LMC120.1	47.44201	11.817	12.761	0.944	3228.24951	0.58	0.397	5.629	0.170	4.746	3221.44380	1.05	0.472	5.000	0.214	3.657	69	70
OGLE-LMC-CEP-0992	5 <sup>h</sup> 07 <sup>m</sup> 16.0 <sup>s</sup>	-68°53'01"	LMC118.1	52.91005	11.294	12.146	0.852	3230.20460	0.22	0.207	5.390	0.022	4.792	3228.20959	0.40	0.201	4.980	0.045	3.959	73	65
OGLE-LMC-CEP-0999	5 <sup>h</sup> 07 <sup>m</sup> 20.1 <sup>s</sup>	-70°27'15"	LMC121.2	26.34352	12.371	13.272	0.901	3218.57167	0.77	0.410	4.973	0.291	3.561	3218.40084	1.33	0.367	4.582	0.233	2.564	49	57
OGLE-LMC-CEP-1100	5 <sup>h</sup> 09 <sup>m</sup> 04.4 <sup>s</sup>	-70°21'54"	LMC113.6	13.63290	13.359	14.185	0.826	3224.43455	0.44	0.167	4.636	0.158	1.822	3238.02595	0.76	0.173	4.203	0.122	0.890	67	63
OGLE-LMC-CEP-1113	5 <sup>h</sup> 09 <sup>m</sup> 20.1 <sup>s</sup>	-70°27'27"	LMC113.7	37.55354	11.917	12.760	0.843	3203.78032	0.61	0.434	5.326	0.221	4.270	3203.60447	1.09	0.465	4.724	0.221	3.204	66	64
OGLE-LMC-CEP-1290	5 <sup>h</sup> 13 <sup>m</sup> 53.7 <sup>s</sup>	-67°03'49"	LMC107.1	48.44961	11.648	12.590	0.942	3221.34724	0.62	0.390	5.435	0.232	4.464	3221.23847	1.12	0.452	4.838	0.229	3.430	52	47
OGLE-LMC-CEP-1591	5 <sup>h</sup> 19 <sup>m</sup> 30.5 <sup>s</sup>	-68°41'10"	LMC101.2	118.52453	10.870	12.052	1.182	3234.66069	0.43	0.047	0.095	0.025	0.113	3221.73250	0.70	0.078	5.403	0.063	5.110	57	54
OGLE-LMC-CEP-1632	5 <sup>h</sup> 20 <sup>m</sup> 17.5 <sup>s</sup>	-67°56'53"	LMC102.3	28.19495	12.856	14.012	1.156	3230.04289	0.59	0.306	4.945	0.194	3.273	3229.76823	1.00	0.327	4.400	0.220	2.274	57	57
OGLE-LMC-CEP-1637	5 <sup>h</sup> 20 <sup>m</sup> 23.0 <sup>s</sup>	-69°02'18"	LMC100.4	31.94691	12.282	13.261	0.979	3212.29806	0.71	0.456	5.162	0.303	3.962	3212.24026	1.21	0.469	4.548	0.288	2.948	63	48
OGLE-LMC-CEP-1677	5 <sup>h</sup> 21 <sup>m</sup> 12.5 <sup>s</sup>	-69°03'08"	LMC100.4	23.57602	12.685	13.704	1.019	3220.20153	0.67	0.337	5.035	0.232	3.489	3220.07714	1.09	0.370	4.563	0.223	2.541	65	62
OGLE-LMC-CEP-2253	5 <sup>h</sup> 31 <sup>m</sup> 21.8 <sup>s</sup>	-70°57'25"	LMC171.6	52.37456	11.772	12.826	1.054	3232.39835	0.55	0.337	5.333	0.149	4.297	3231.01078	0.99	0.402	4.743	0.166	3.243	50	49
OGLE-LMC-CEP-2504	5 <sup>h</sup> 35 <sup>m</sup> 36.1 <sup>s</sup>	-68°32'04"	LMC174.6	24.33819	12.388	13.240	0.852	3237.71028	0.68	0.359	4.894	0.262	3.157	3239.88429	0.91	0.280	4.342	0.111	2.241	47	26

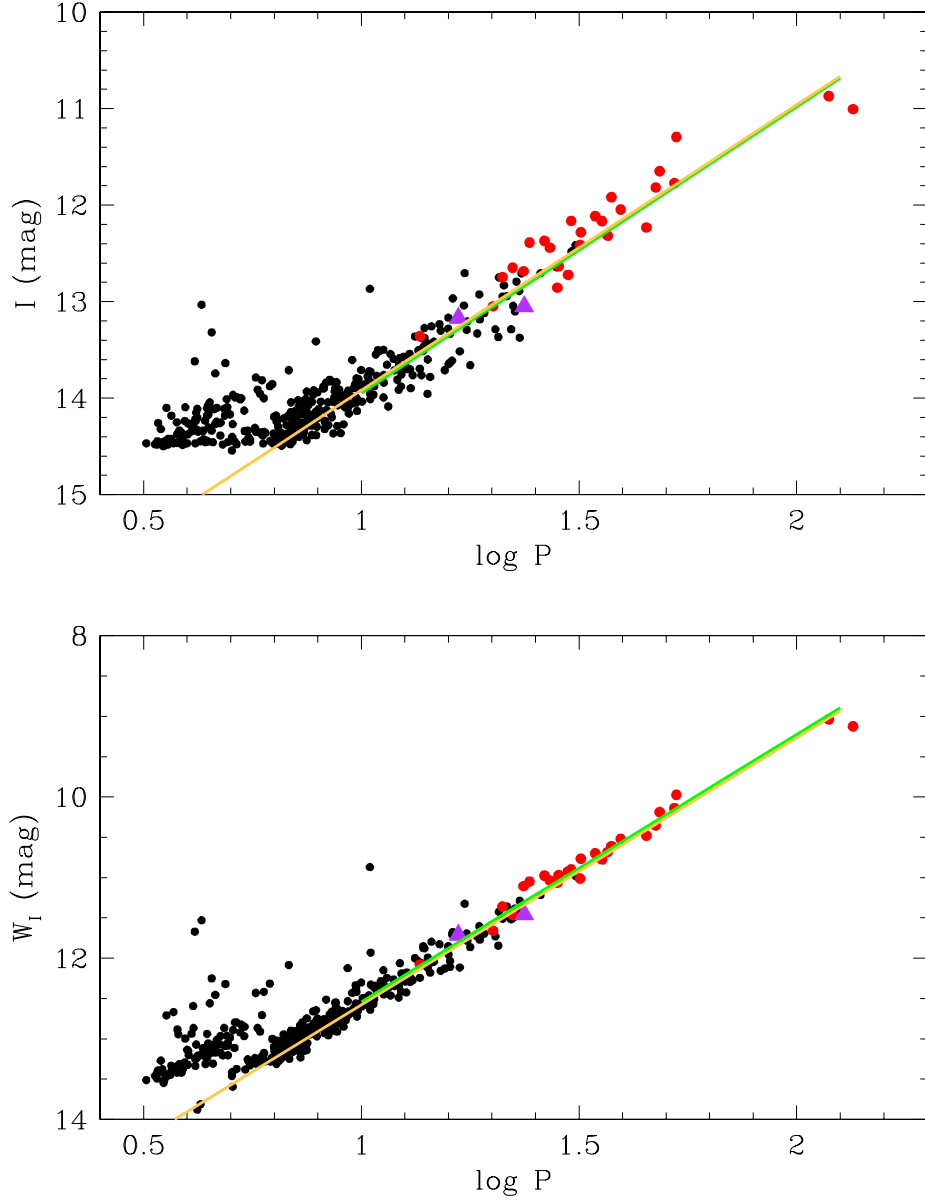


Fig. 7. Period–luminosity diagrams for classical Cepheids. Red points correspond to stars for which new photometry was obtained and violet triangles correspond to newly found objects. Cepheids from the main OGLE-III catalog are marked with black dots. Green line shows the fit for Cepheids with periods above 10 days and yellow line represents relation derived in Soszyński *et al.* (2008). All measurements are from the Shallow Survey.

We used Wesenheit index (Madore 1982) defined as:

$$W_I = I - 1.55 \cdot (V - I). \quad (2)$$

Relations presented in Soszyński *et al.* (2008) for Cepheids of periods below

$\log P = 1.5$  were as follows:

$$\begin{aligned} W_I &= -3.314(\pm 0.009) \log P + 15.893(\pm 0.006) & \sigma &= 0.080 \\ I &= -2.959(\pm 0.016) \log P + 16.879(\pm 0.010) & \sigma &= 0.150 \end{aligned} \quad (3)$$

The results are graphically presented in Fig. 7. Red points correspond to the Cepheids for which new photometry was obtained and newly detected Cepheids are marked with violet triangles. The green line is the relation for Cepheids with periods longer than 10 days and the yellow one is the relation derived in Soszyński *et al.* (2008) paper. One can note that there are no statistically significant deviations in relations for longer period domain. Obviously, we have limited sample of long-period Cepheids in the LMC and, moreover, we did not detect any variables of this type with periods ranging from about 55 days to 115 days.

It is worth noting that mean magnitude scatter for brighter Cepheids is smaller than in the diagrams based on the main OGLE-III photometry (Soszyński *et al.* 2008). This effect, specifically visible for  $\log P > 1.2$ , can be caused by non-linear CCD response close to the saturation limit and/or by imperfections in DIA subtraction procedures for luminous stars. We also checked that significant color index shifts for some objects are caused by stronger blending in the Shallow Survey images in comparison to the regular OGLE-III data.

## 5. RR Lyr Variables

In the magnitude range of the Shallow Survey searched for variables, the main OGLE-III catalog (Soszyński *et al.* 2009a) contains ten RR Lyr stars located in the observed fields. We identified one new RR Lyr variable at equatorial coordinates:  $RA = 5^h 03^m 01^s.3$ ,  $DEC = -69^\circ 09' 01''$ . Considering its brightness it must be a foreground Galactic object. Despite of the fact that the star is saturated in the OGLE-III database we were able to calculate its proper motion based on the extracted DOPHOT positions data derived in the main OGLE-III survey :

$$\begin{aligned} \mu_\delta &= 8.17 \pm 0.32 \text{ mas/yr} \\ \mu_\alpha \cos \delta &= 10.06 \pm 0.32 \text{ mas/yr} \end{aligned}$$

We applied the method presented by Poleski *et al.* (2012). The proper motion was appropriately corrected so the resultant proper motion of all LMC stars was equal 0 with an error of 0.25 mas/yr. No parallax effect was visible.

Also we added to our catalog two RR Lyr stars which were already known – both are present in the ASAS catalog (Pojmański 2002) and one also has XX Dor designation. The basic data for new RR Lyr stars are presented in the OGLE Internet Archive in table of the same format as for Cepheids. The last extra column contains cross-identification designations. Fig. 8 shows *I*- and *V*-band light curves for those stars.

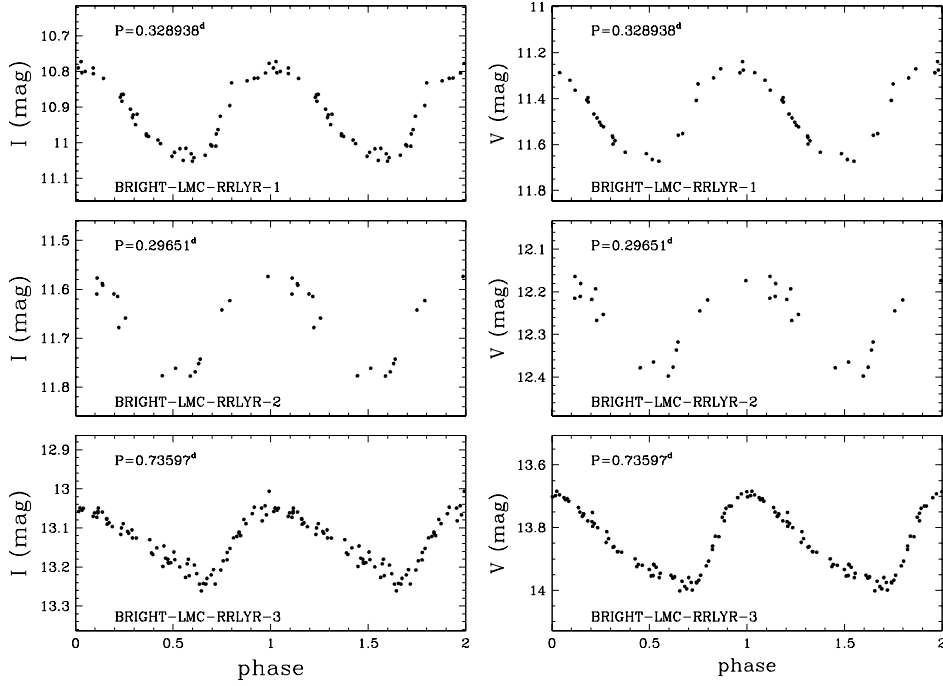


Fig. 8. New Galactic RR Lyr variables added to the OGLE-III catalog.

## 6. Eclipsing Variables

We updated eclipsing variables catalog with 82 new objects. The main OGLE-III catalog was focused on detached binaries (Graczyk *et al.* 2011) so it is not surprising that we found many contact (EW) or semi-detached systems (EB). We also discovered 32 ellipsoidal variables for which eclipses are observed or not. Six objects were already present in the ASAS catalog (Szczygieł *et al.* 2010).

Table 2 lists new eclipsing binaries. Subsequent columns contain the following data: (1) variable star identification label, (2,3) equatorial coordinates J2000.0, (4) subfield designation, (5) period, (6) *I*-band mean magnitude, (7) *V*-band mean magnitude, (8) (*V*-*I*) color index, (9,10) number of observations in the *I*- and *V*-band, (11,12) dispersion of magnitudes for the *I*- and *V*-band, (13) subtype, (14) designations in other catalogs/surveys: ASAS (no prefix, Pojmański 2002), 2MASS (Cutri *et al.* 2003), HV (Payne-Gaposchkin 1971), HD (Cannon 1925), Spitzer – SSTISAGE1C (Vijh *et al.* 2009) and SSTISAGEMC (Meixner *et al.* 2006), MA-CHO (Ochsenbein, Bauer and Marcout 2000), UCAC2 (Zacharias *et al.* 2004), [BE74] (Bohannon and Epps 1974), [FBM2009] (Fariña *et al.* 2009), [L72] (Massey 2000), NGC 2070 MEL (Melnick 1985). The subtypes were assigned based on light curve shape. Fig. 9 presents color–magnitude diagram with positions of detected eclipsing binaries.

Table 2

The first 25 lines of eclipsing variable stars catalog

ID	RA (J2000.0)	DEC (J2000.0)	Subfield	Period [days]	$I$ [mag]	$V$ [mag]	$V-I$ [mag]	$N_I$	$N_V$	$\sigma_I$ [mag]	$\sigma_V$ [mag]	Subtype	Other designations
BRIGHT-LMC-ECL-01	5 <sup>h</sup> 18 <sup>m</sup> 32 <sup>s</sup> .6	−68°13′32″	LMC102.8	0.285464	10.133	11.108	0.975	45	55	0.188	0.203	EW	051832-6813.6
BRIGHT-LMC-ECL-02	4 <sup>h</sup> 59 <sup>m</sup> 54 <sup>s</sup> .6	−70°48′45″	LMC130.4	0.406400	13.109	13.724	0.616	47	59	0.072	0.065	EB	–
BRIGHT-LMC-ECL-03	5 <sup>h</sup> 28 <sup>m</sup> 32 <sup>s</sup> .5	−68°36′14″	LMC167.6	0.576860	10.473	11.336	0.863	43	39	0.048	0.040	EB/EA	052833-6836.2
BRIGHT-LMC-ECL-04	4 <sup>h</sup> 59 <sup>m</sup> 05 <sup>s</sup> .8	−69°31′50″	LMC127.8	0.579960	13.302	13.746	0.444	32	43	0.059	0.060	EW	–
BRIGHT-LMC-ECL-05	6 <sup>h</sup> 05 <sup>m</sup> 22 <sup>s</sup> .0	−69°47′00″	LMC206.6	0.593020	11.690	12.244	0.554	17	17	0.076	0.077	EW	060521-6947.1
BRIGHT-LMC-ECL-06	5 <sup>h</sup> 55 <sup>m</sup> 36 <sup>s</sup> .1	−70°13′07″	LMC192.4	0.789600	12.344	13.021	0.678	50	40	0.049	0.057	EB	–
BRIGHT-LMC-ECL-07	5 <sup>h</sup> 18 <sup>m</sup> 25 <sup>s</sup> .6	−69°12′13″	LMC100.6	1.062028	14.449	14.247	−0.202	64	59	0.056	0.052	EW	2MASS J05182564-6912128
BRIGHT-LMC-ECL-08	5 <sup>h</sup> 35 <sup>m</sup> 02 <sup>s</sup> .1	−68°43′45″	LMC174.7	1.086410	12.048	12.152	0.103	57	58	0.095	0.047	EA	053503-6843.7
BRIGHT-LMC-ECL-09	5 <sup>h</sup> 38 <sup>m</sup> 28 <sup>s</sup> .5	−69°11′19″	LMC175.6	1.124180	14.385	14.485	0.100	36	28	0.094	0.105	EW	–
BRIGHT-LMC-ECL-10	5 <sup>h</sup> 10 <sup>m</sup> 27 <sup>s</sup> .1	−67°54′56″	LMC109.6	1.127451	14.130	13.967	−0.162	30	31	0.061	0.079	EW	HV 5623
BRIGHT-LMC-ECL-11	4 <sup>h</sup> 55 <sup>m</sup> 11 <sup>s</sup> .4	−69°22′31″	LMC135.2	1.238320	14.331	14.139	−0.192	67	64	0.037	0.038	EW	–
BRIGHT-LMC-ECL-12	5 <sup>h</sup> 10 <sup>m</sup> 29 <sup>s</sup> .2	−69°19′16″	LMC111.7	1.251180	13.794	14.273	0.479	30	8	0.446	0.909	EB	–
BRIGHT-LMC-ECL-13	5 <sup>h</sup> 35 <sup>m</sup> 17 <sup>s</sup> .9	−68°52′50″	LMC174.8	1.255580	14.190	15.258	1.068	47	19	0.056	0.149	EB	MACHO 82.8894.18
BRIGHT-LMC-ECL-14	5 <sup>h</sup> 37 <sup>m</sup> 30 <sup>s</sup> .9	−69°11′07″	LMC175.6	1.327192	14.011	14.617	0.607	59	54	0.052	0.053	EW	2MASS J05373092-6911070
BRIGHT-LMC-ECL-15	5 <sup>h</sup> 04 <sup>m</sup> 51 <sup>s</sup> .5	−70°42′36″	LMC121.8	1.383040	14.293	14.088	−0.205	69	66	0.021	0.020	EII	–
BRIGHT-LMC-ECL-16	5 <sup>h</sup> 27 <sup>m</sup> 54 <sup>s</sup> .1	−68°59′45″	LMC161.4	1.396120	14.384	14.283	−0.101	61	59	0.044	0.039	EII	–
BRIGHT-LMC-ECL-17	5 <sup>h</sup> 34 <sup>m</sup> 41 <sup>s</sup> .4	−69°31′39″	LMC168.1	1.404800	13.885	13.850	−0.036	37	41	0.129	0.128	EW	MACHO 81.8763.8
BRIGHT-LMC-ECL-18	5 <sup>h</sup> 06 <sup>m</sup> 00 <sup>s</sup> .3	−70°40′54″	LMC121.1	1.668340	13.614	15.306	1.692	23	5	0.644	0.320	EW	–
BRIGHT-LMC-ECL-19	5 <sup>h</sup> 05 <sup>m</sup> 11 <sup>s</sup> .9	−70°11′20″	LMC121.5	1.698480	14.213	13.963	−0.250	57	46	0.032	0.031	EII	–
BRIGHT-LMC-ECL-20	4 <sup>h</sup> 49 <sup>m</sup> 51 <sup>s</sup> .4	−69°12′04″	LMC135.6	1.736348	12.596	12.541	−0.056	63	66	0.030	0.031	EW	2MASS J04495141-6912043
BRIGHT-LMC-ECL-21	5 <sup>h</sup> 37 <sup>m</sup> 59 <sup>s</sup> .5	−69°09′02″	LMC175.6	1.855280	13.711	13.744	0.033	59	56	0.029	0.020	EII	2MASS J05375943-6909010
BRIGHT-LMC-ECL-22	5 <sup>h</sup> 40 <sup>m</sup> 20 <sup>s</sup> .6	−69°39′01″	LMC176.4	1.871260	14.477	14.461	−0.016	58	58	0.044	0.042	EW	[FBM2009] 107
BRIGHT-LMC-ECL-23	5 <sup>h</sup> 28 <sup>m</sup> 60 <sup>s</sup> .0	−68°49′27″	LMC167.8	1.902040	14.332	14.182	−0.150	41	17	0.041	0.037	EII	SSTISAGEMC J052859.98-684926.5
BRIGHT-LMC-ECL-24	4 <sup>h</sup> 54 <sup>m</sup> 27 <sup>s</sup> .5	−68°33′52″	LMC134.3	2.001460	12.700	13.470	0.770	78	69	0.014	0.019	EII	–
BRIGHT-LMC-ECL-25	5 <sup>h</sup> 06 <sup>m</sup> 29 <sup>s</sup> .0	−70°37′51″	LMC121.1	2.176380	14.271	14.058	−0.213	63	57	0.072	0.071	EW	–

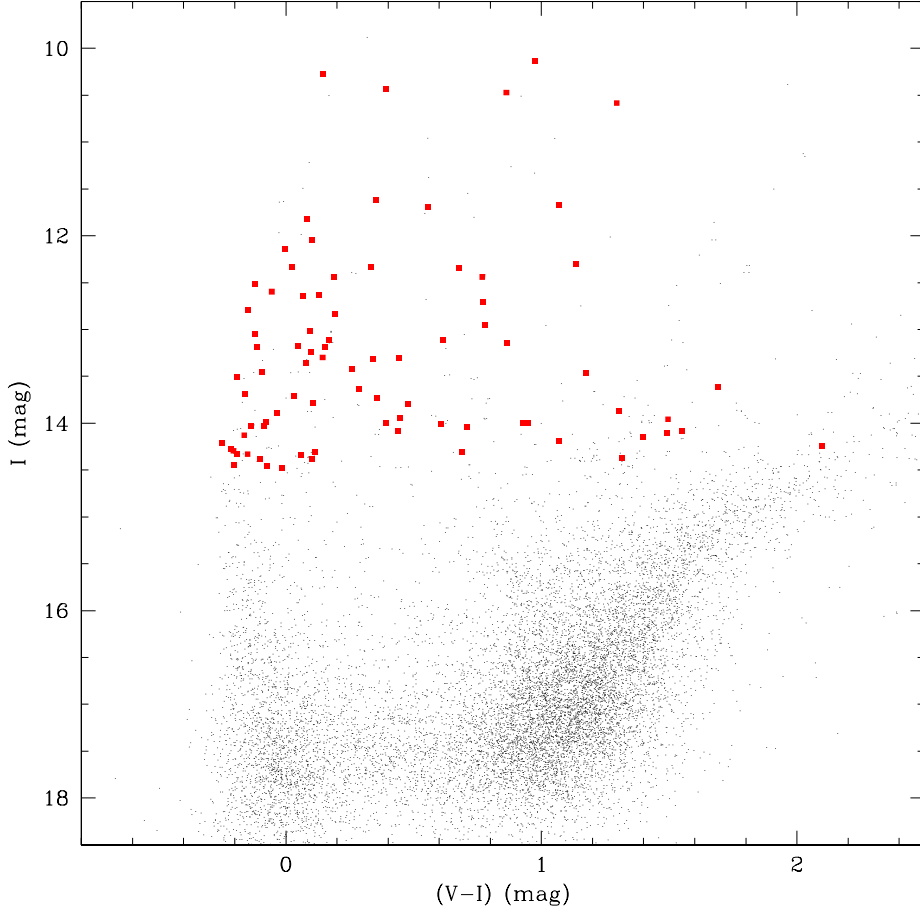


Fig. 9. Color-magnitude diagram for eclipsing stars (red) added to the OGLE-III catalog from Shallow Survey data. Black dots represent all stars from the LMC100.1 subfield.

## 7. Miras and Semiregular Variables

Amongst red giants eight new Miras and 102 semiregular variables (SRV) were found. They belong to the broad category of Long-Period Variables (LPV). The cross-identification with other catalogs shows that three classified Miras were already found while four other objects were recognized as variable stars. Compared to the main OGLE-III catalog (consisting of 12 795 objects in the full magnitudes range) this sample is very small so it cannot affect noticeably already conducted analysis (Soszyński *et al.* 2009b), especially as stars of those types split into several groups with different luminosity-period relations. Where possible each star was cross-identified with 2MASS Survey infrared counterparts (Cutri *et al.* 2003).

In Fig. 10 color-magnitude diagram is presented with cyan points representing SRV stars and red points representing Miras. Part of the catalog with basic data for those objects is presented in Table 3. The columns contain following data: (1) variable star identification label, (2,3) equatorial coordinates J2000.0, (4) sub-

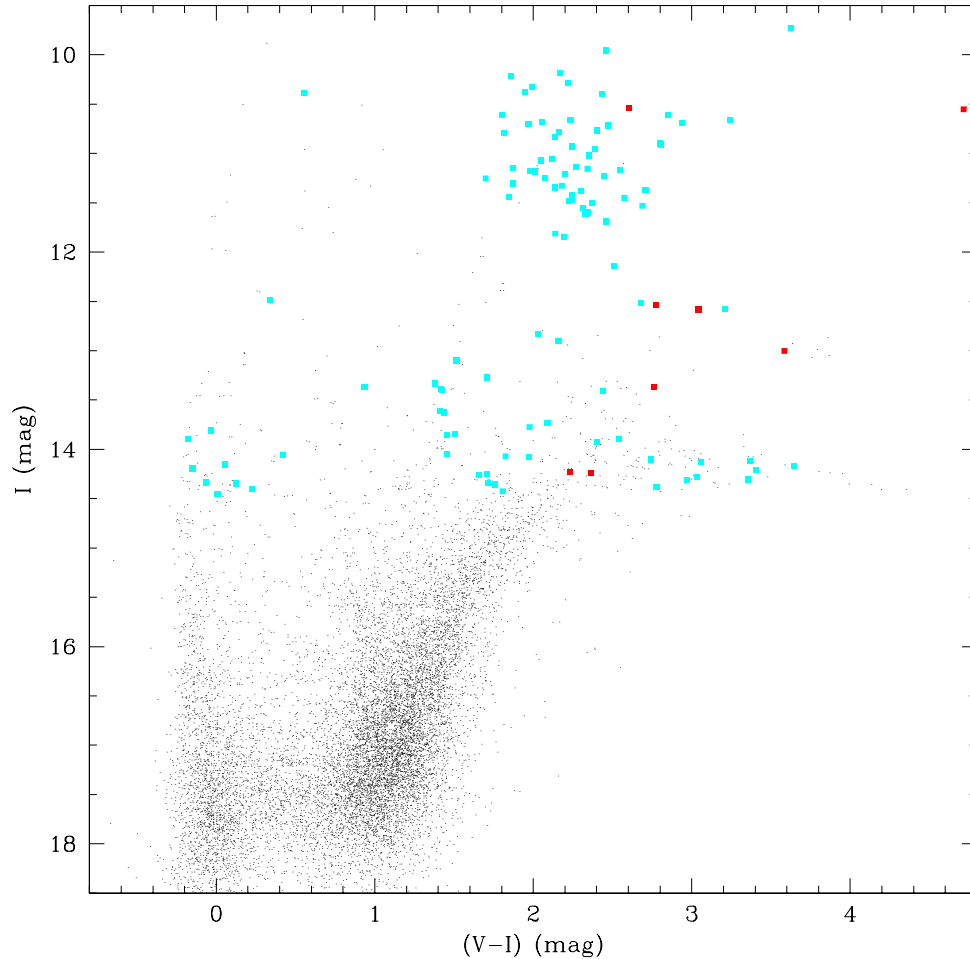


Fig. 10. Color-magnitude diagram for long-period variables. Red points represent Miras and cyan points correspond to SRV stars. Black dots represent all stars from the LMC100.1 subfield.

field designation, (5) dominant period, (6) *I*-band mean magnitude, (7) *V*-band mean magnitude, (8) (*V-I*) color index, (9,10) number of observations in the *I*- and *V*-band, (11,12) dispersion of magnitudes for the *I*- and *V*-band, (13) subtype, (14-17) 2MASS object cross-identification: separation distance and *JKH* infrared photometry, (18) designations in other catalogs/surveys (the same as for eclipsing variables). Fig. 11 shows *I*-band light curves for new Miras.

Table 3  
First 25 lines of long-period variable stars catalog

ID	RA (J2000.0)	DEC (J2000.0)	Subfield	Period [days]	<i>I</i> [mag]	<i>V</i> [mag]	<i>V</i> − <i>I</i> [mag]	<i>N<sub>I</sub></i>	<i>N<sub>V</sub></i>	$\sigma_I$ [mag]	$\sigma_V$ [mag]	Subtype	d [arcsec]	J [mag]	H [mag]	K [mag]	Other designations
BRIGHT-LMC-LPV-001	5 <sup>h</sup> 24 <sup>m</sup> 04 <sup>s</sup> .7	−70°33′10″	LMC163.7	178.571430	14.233	16.464	2.231	38	19	0.390	0.719	MIRA	1.35	12.992	12.189	11.783	–
BRIGHT-LMC-LPV-002	5 <sup>h</sup> 25 <sup>m</sup> 11 <sup>s</sup> .6	−68°42′44″	LMC160.7	248.138960	12.578	15.619	3.041	42	17	0.390	0.606	MIRA	0.40	10.307	9.395	9.026	2MASS J05251160-6842444
BRIGHT-LMC-LPV-003	4 <sup>h</sup> 36 <sup>m</sup> 46 <sup>s</sup> .8	−70°18′41″	LMC151.6	250.000000	10.552	15.268	4.716	25	22	0.777	1.823	MIRA	0.04	7.729	6.917	6.500	043648-7018.6
BRIGHT-LMC-LPV-004	5 <sup>h</sup> 15 <sup>m</sup> 47 <sup>s</sup> .4	−70°04′33″	LMC112.1	261.780100	14.236	16.598	2.362	63	24	0.713	0.727	MIRA	1.47	12.442	11.595	11.193	–
BRIGHT-LMC-LPV-005	5 <sup>h</sup> 39 <sup>m</sup> 56 <sup>s</sup> .9	−69°35′21″	LMC176.4	416.739126	12.541	15.312	2.770	59	52	0.413	0.890	MIRA	0.29	10.759	9.900	9.589	HV 2763
BRIGHT-LMC-LPV-006	5 <sup>h</sup> 27 <sup>m</sup> 10 <sup>s</sup> .2	−69°36′27″	LMC162.4	512.170000	13.004	16.587	3.583	55	19	0.881	1.026	MIRA	0.31	10.399	9.544	9.159	HV 12048
BRIGHT-LMC-LPV-007	5 <sup>h</sup> 40 <sup>m</sup> 32 <sup>s</sup> .8	−71°31′59″	LMC179.6	625.000000	13.367	16.128	2.762	52	11	0.745	1.041	MIRA	0.15	10.224	9.349	8.829	2MASS J05403279-7131591
BRIGHT-LMC-LPV-008	5 <sup>h</sup> 30 <sup>m</sup> 41 <sup>s</sup> .4	−69°15′34″	LMC168.7	669.230782	10.540	13.147	2.607	38	44	0.412	0.805	MIRA	0.31	8.752	7.993	7.591	053041-6915.5
BRIGHT-LMC-LPV-009	5 <sup>h</sup> 08 <sup>m</sup> 21 <sup>s</sup> .3	−67°55′18″	LMC117.3	75.757580	13.735	15.824	2.089	21	17	0.043	0.087	SRV	1.40	12.161	11.207	10.925	–
BRIGHT-LMC-LPV-010	5 <sup>h</sup> 31 <sup>m</sup> 22 <sup>s</sup> .8	−69°02′30″	LMC168.5	82.987550	14.457	14.463	0.006	57	56	0.046	0.035	SRV	0.28	14.407	14.558	14.594	MACHO 82.8286.14
BRIGHT-LMC-LPV-011	5 <sup>h</sup> 05 <sup>m</sup> 29 <sup>s</sup> .7	−69°00′27″	LMC119.5	97.087380	13.926	16.326	2.400	63	58	0.090	0.196	SRV	–	–	–	–	–
BRIGHT-LMC-LPV-012	5 <sup>h</sup> 15 <sup>m</sup> 41 <sup>s</sup> .0	−69°01′10″	LMC111.4	107.526880	14.042	15.495	1.453	73	42	0.033	0.036	SRV	0.41	13.051	12.342	12.202	2MASS J05154103-6901096
BRIGHT-LMC-LPV-013	5 <sup>h</sup> 30 <sup>m</sup> 18 <sup>s</sup> .5	−70°26′41″	LMC170.7	107.526880	14.338	16.051	1.714	52	23	0.031	0.059	SRV	0.20	13.160	12.389	12.129	2MASS J05301846-7026411
BRIGHT-LMC-LPV-014	5 <sup>h</sup> 30 <sup>m</sup> 10 <sup>s</sup> .3	−69°00′46″	LMC168.5	109.890110	14.260	15.914	1.654	38	19	0.041	0.063	SRV	0.04	13.079	12.300	12.094	2MASS J05301027-6900460
BRIGHT-LMC-LPV-015	5 <sup>h</sup> 29 <sup>m</sup> 46 <sup>s</sup> .2	−68°37′03″	LMC167.6	113.895220	11.328	13.509	2.181	30	39	0.047	0.088	SRV	0.56	9.897	9.034	8.747	2MASS J05294618-6837024
BRIGHT-LMC-LPV-016	4 <sup>h</sup> 53 <sup>m</sup> 44 <sup>s</sup> .4	−69°22′54″	LMC135.2	114.547540	13.844	15.347	1.502	72	60	0.221	0.034	SRV	0.45	12.692	11.969	11.811	2MASS J04534436-6922535
BRIGHT-LMC-LPV-017	5 <sup>h</sup> 10 <sup>m</sup> 32 <sup>s</sup> .6	−69°50′44″	LMC112.7	121.951220	14.245	15.952	1.707	26	13	0.311	0.241	SRV	–	–	–	–	–
BRIGHT-LMC-LPV-018	4 <sup>h</sup> 58 <sup>m</sup> 04 <sup>s</sup> .0	−71°09′11″	LMC130.2	131.578950	12.516	15.196	2.679	41	25	0.049	0.100	SRV	0.18	10.978	10.007	9.748	2MASS J04580400-7109108
BRIGHT-LMC-LPV-019	5 <sup>h</sup> 40 <sup>m</sup> 17 <sup>s</sup> .5	−69°30′57″	LMC175.1	138.312590	10.390	10.944	0.554	58	50	0.028	0.033	SRV	0.46	9.902	9.721	9.581	2MASS J05401751-6930574
BRIGHT-LMC-LPV-020	5 <sup>h</sup> 23 <sup>m</sup> 48 <sup>s</sup> .0	−70°07′35″	LMC162.8	140.056020	11.814	13.953	2.138	41	30	0.033	0.078	SRV	0.36	10.407	9.545	9.269	2MASS J05234794-7007348
BRIGHT-LMC-LPV-021	4 <sup>h</sup> 49 <sup>m</sup> 46 <sup>s</sup> .8	−69°23′14″	LMC135.7	144.717800	11.844	14.041	2.197	74	70	0.039	0.117	SRV	0.17	10.364	9.470	9.159	–
BRIGHT-LMC-LPV-022	5 <sup>h</sup> 32 <sup>m</sup> 58 <sup>s</sup> .3	−69°55′51″	LMC169.2	155.521000	13.406	15.846	2.440	56	52	0.052	0.092	SRV	0.64	11.540	10.539	10.203	2MASS J05325832-6955503
BRIGHT-LMC-LPV-023	5 <sup>h</sup> 37 <sup>m</sup> 05 <sup>s</sup> .9	−69°52′00″	LMC176.7	161.290320	14.078	16.051	1.972	30	27	0.064	0.111	SRV	0.50	12.739	11.842	11.583	2MASS J05370582-6951598
BRIGHT-LMC-LPV-024	5 <sup>h</sup> 37 <sup>m</sup> 20 <sup>s</sup> .5	−69°19′39″	LMC175.7	162.601630	10.704	12.676	1.972	59	56	0.032	0.063	SRV	0.36	9.418	8.541	8.278	2MASS J05372049-6919386
BRIGHT-LMC-LPV-025	5 <sup>h</sup> 08 <sup>m</sup> 59 <sup>s</sup> .7	−68°35′36″	LMC118.3	164.744650	14.423	16.230	1.807	73	66	0.029	0.055	SRV	0.69	13.198	12.294	12.079	–



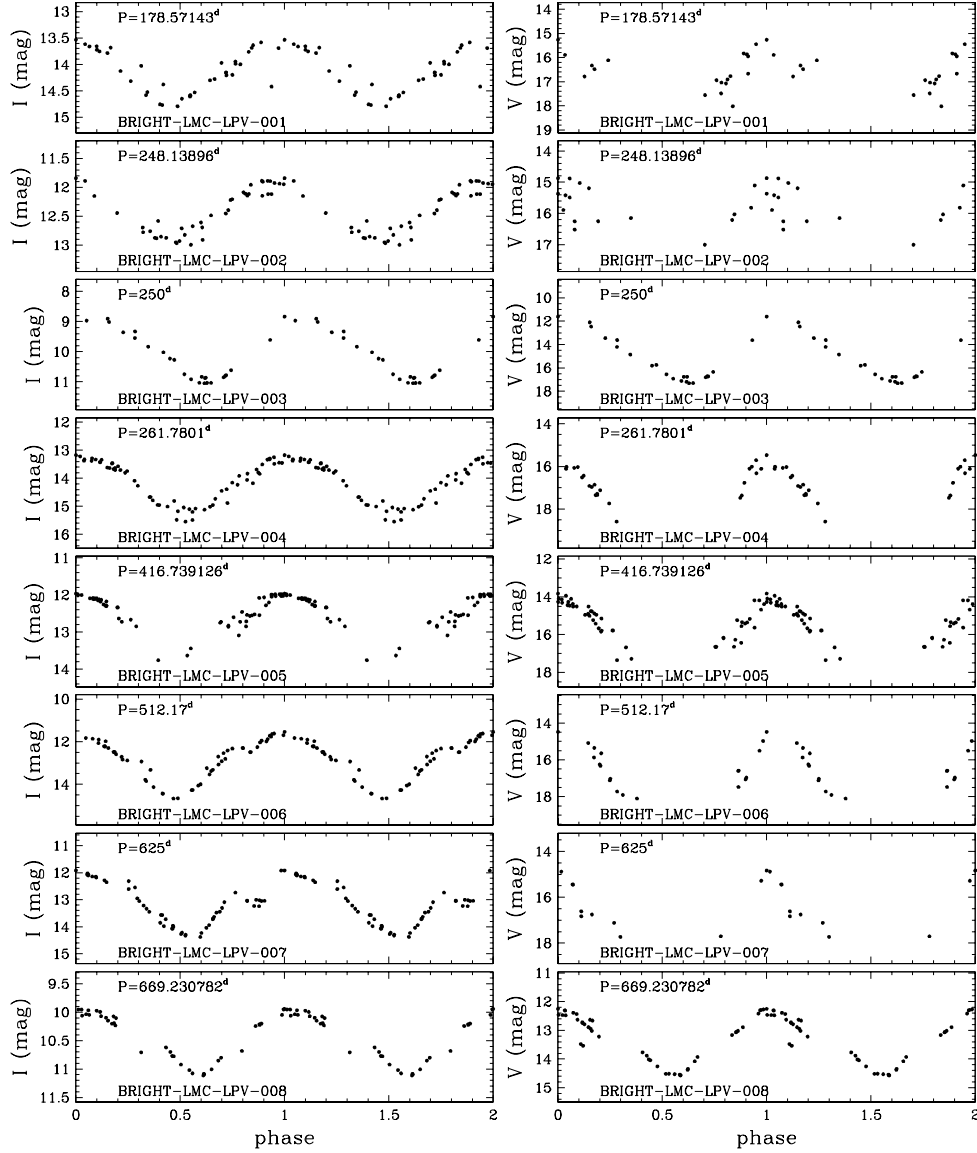


Fig. 11. VI-band light curves for new Miras.

## 8. Miscellaneous Variables

The most numerous group of variable stars in our sample constitute stars for which we could not clearly determine periodicity. We found 558 such objects. Due to limited observational epochs it is possible we were not able to distinguish some, in fact, periodic variable stars. Long-period variables often require observations in long timescales to establish the nature of their brightness fluctuations. This condition is fulfilled by OGLE project data (now it is over 20 years of regular survey)

but unfortunately Shallow Survey spanned for 4.5 years only and for some fields only 13 epochs were collected. However in this way we show which stars can be particularly interesting for further follow-up observations. In order to have a broader view of our sample we prepared color–magnitude diagram (Fig. 12) with color-coded “amplitudes” (differences between maximum and minimum magnitudes after removal of  $3\sigma$  deviating points). One can notice that bigger-amplitude variables concentrate in two regions of the CMD. We also checked that variables do not separate on Wesenheit indices  $W_I - W_{JK}$  plane (Fig. 13), what takes place in case of long-period variables.

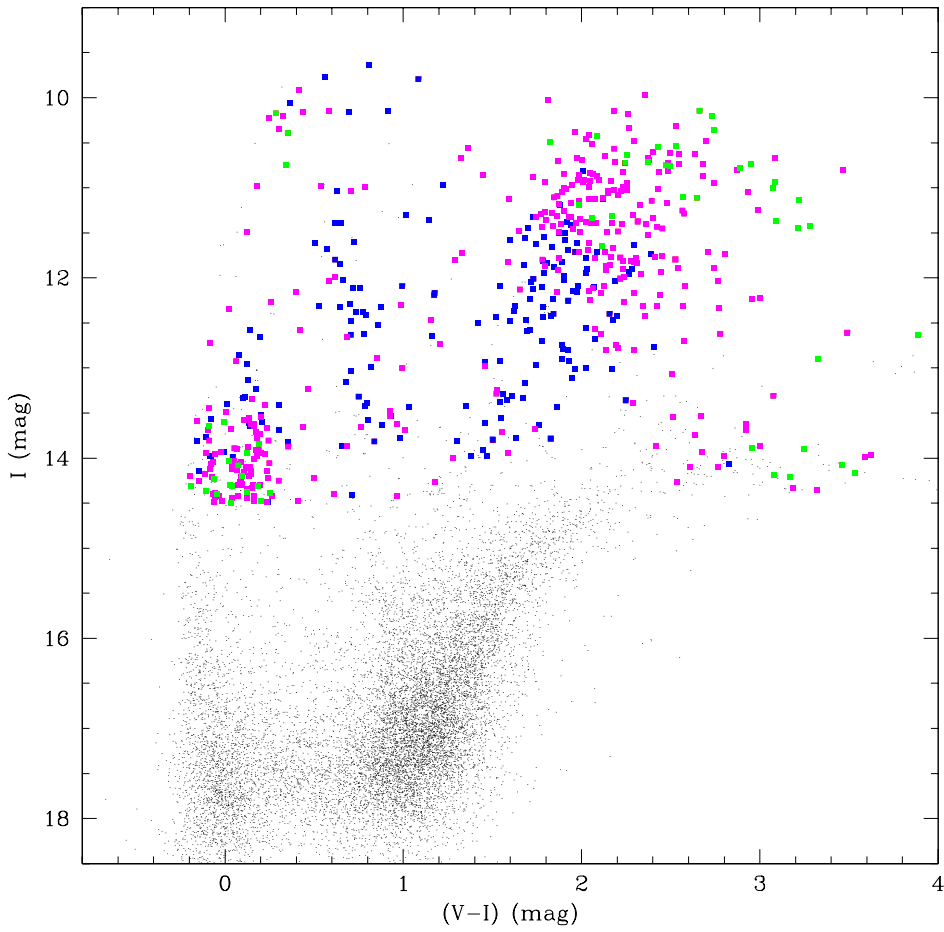


Fig. 12. Color–magnitudes diagram for miscellaneous variables. Amplitudes are color-coded: blue –  $\text{amp} \leq 0.1$  mag, magenta –  $0.1 \text{ mag} < \text{amp} \leq 0.5$  mag, green –  $\text{amp} > 0.5$  mag. Black dots represent all stars from the LMC100.1 subfield.

Basic parameters for those stars are presented in OGLE Internet Archive in the same manner as for long-period variables with the “period” column omitted.

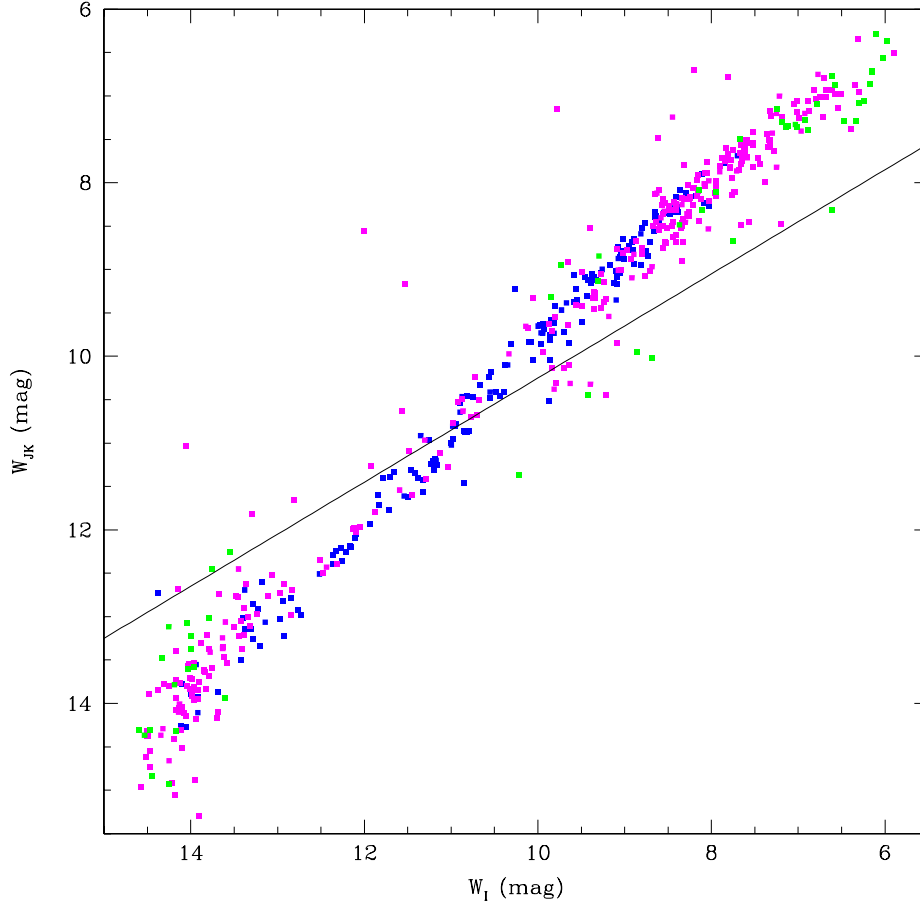


Fig. 13. Wesenheit indices diagram for miscellaneous variables cross-identified with 2MASS catalog.  $W_{JK}$  denotes infrared Wesenheit index defined as  $W_{JK} = J - 0.686 \cdot (J - K)$ . Amplitudes are color-coded: blue –  $\text{amp} \leq 0.1$  mag, magenta –  $0.1 \text{ mag} < \text{amp} \leq 0.5$  mag, green –  $\text{amp} > 0.5$  mag. Black line represents approximate separation border between oxygen-rich and carbon-rich stars based on data from Soszyński *et al.* (2009b).

## 9. Discussion

The data from the Shallow Survey allowed us to extend period–luminosity relation for classical Cepheids in the Large Magellanic Cloud up to 134 days. In that range we did not observe any deviations from linearity. However, this conclusion is a little weakened due to the presence of only two Cepheids with periods above 53 days in our sample. Therefore we cannot confirm recent suggestion that for long-period Cepheids ( $P > 100$  d) luminosity is period-independent (Bird *et al.* 2009) neither lack of such a flattening (Fiorentino *et al.* 2012). We have also updated long-period variables and eclipsing binaries catalogs with new objects of

luminosities up to 9.7 mag. The selected sample of miscellaneous stars of suspected irregular variability is worth performing follow-up observations. It is still an open question if red giants can pulsate in strictly irregular manner.

The fact that we have not found significant number of new regular variable stars proves that the OGLE-III catalogs are very complete. Variable stars were omitted mainly in specific situations – like a saturation of the star itself or its location near other saturated object.

## 10. Data Availability

The described supplementary catalogs of bright variable stars in the LMC and their photometry are available to the astronomical community from the OGLE Internet Archive:

<http://ogle.astrouw.edu.pl>  
[ftp://ftp.astrouw.edu.pl/ogle/ogle3/OIII-CVS/bright\\_lmc/](ftp://ftp.astrouw.edu.pl/ogle/ogle3/OIII-CVS/bright_lmc/)

**Acknowledgements.** The OGLE project has received funding from the European Research Council under the European Community’s Seventh Framework Programme (FP7/2007-2013)/ERC grant agreement no. 246678 to AU. This paper was partially supported by Polish grant N N203 510038. We gratefully acknowledge financial support for this work from the Chilean Center for Astrophysics FON-DAP 15010003, and from the BASAL Centro de Astrofísica y Tecnologías Afines (CATA) PFB-06/2007.

## REFERENCES

- Bird, J.C., Stanek, K.Z., and Prieto, J.L. 2009, *ApJ*, **695**, 874.  
 Bohannan, B., and Epps, H. W. 1974, *A&AS*, **18**, 47.  
 Cannon, A. J. 1925, *Annals of Harvard College Observatory*, **100**, 17.  
 Cutri, R.M., *et al.* 2003, “2MASS All-Sky Point Source Catalog”, NASA/IPAC Infrared Science Archive.  
 Fariña, C., Bosch, G. L., Morrell, N. I., Barbá, R. H., and Walborn, N. R. 2009, *AJ*, **138**, 510.  
 Fiorentino, G., *et al.* 2012, *Astrophys. and Space Sci.*, **341**, 143.  
 Graczyk, D., Soszyński, I., Poleski, R., Pietrzyński, G., Udalski, A., Szymański, M. K., Kubiak, M., Wyrzykowski, Ł., and Ulaczyk, K. 2011, *Acta Astron.*, **61**, 103.  
 Madore, B.F. 1982, *ApJ*, **253**, 575.  
 Massey, P., Waterhouse, E., and DeGioia-Eastwood, K. 2000, *AJ*, **119**, 2214.  
 Meixner, M., Gordon, K. D., Indebetouw, R., *et al.* 2006, *AJ*, **132**, 2268.  
 Melnick, J. 1985, *A&A*, **153**, 235.  
 Ochsenbein, F., Bauer, P., and Marcout, J. 2000, *A&AS*, **143**, 23.  
 Payne-Gaposchkin, C.H. 1971, *Smithsonian Contrib. Astrophys.*, **13**.  
 Pojmański, G. 2002, *Acta Astron.*, **52**, 397.  
 Poleski, R., Soszyński, I., Udalski, A., Szymański, M.K., Kubiak, M., Pietrzyński, G., Wyrzykowski, Ł., Ulaczyk, K. 2012, *Acta Astron.*, **62**, 1.  
 Soszyński, I., Poleski, R., Udalski, A., Szymański, M.K., Kubiak, M., Pietrzyński, G., Wyrzykowski, Ł., Szewczyk, O., and Ulaczyk, K. 2008, *Acta Astron.*, **58**, 163.

- Soszyński, I., Udalski, A., Szymański, M.K., Kubiak, M., Pietrzyński, G., Wyrzykowski, Ł., Szewczyk, O., Ulaczyk, K., and Poleski, R. 2009a, *Acta Astron.*, **59**, 1.
- Soszyński, I., Udalski, A., Szymański, M.K., Kubiak, M., Pietrzyński, G., Wyrzykowski, Ł., Szewczyk, O., Ulaczyk, K., and Poleski, R. 2009b, *Acta Astron.*, **59**, 239.
- Szczygieł, D.M., Stanek, K.Z., Bonanos, A.Z., Pojmański, G., Pilecki, B., and Prieto, J.L. 2010, *AJ*, **140**, 14.
- Szymański, M., Udalski, A., Soszyński, I., Kubiak, M., Pietrzyński, G., Poleski, R., Wyrzykowski, Ł., and Ulaczyk, K. 2011, *Acta Astron.*, **61**, 83.
- Udalski, A. 2003, *Acta Astron.*, **53**, 291.
- Ulaczyk, K., Szymański, M.K., Udalski, A., Kubiak, M., Pietrzyński, G., Soszyński, I., Wyrzykowski, Ł., Poleski, R., Gieren, W., Walker, A. R., and Garcia-Varela, A. 2012, *Acta Astron.*, **62**, 247.
- Vijh, U. P., Meixner, M., Babler, B., *et al.* 2009, *AJ*, **137**, 3139.
- Zacharias, N., Urban, S. E., Zacharias, M. I., *et al.* 2004, *AJ*, **127**, 3043.